ELSEVIER

International Journal of Heat and Fluid Flow 20 (1999) 172–184

International Journal of HEAT AND FLUID FLOW

Computation of turbulent buoyant flows in enclosures with low-Reynolds-number k-ω models

Shia-Hui Peng [a,b], Lars Davidson [a,*]

[a] Thermo and Fluid Dynamics, Chalmers University of Technology, S-412 96 Gothenburg, Sweden
[b] Work Organization and Technology, National Institute for Working Life, S-171 84 Solna, Sweden

Received 25 November 1997; accepted 2 October 1998

Abstract

This work deals with the computation of turbulent buoyant convection flows with thermal stratification using the low-Reynolds-number (LRN) k-ω model. When applying the k-ε model to buoyancy-driven cavity flows induced by differentially heated side walls, a problem commonly encountered at moderate Rayleigh numbers ($Ra = 10^{10} - 10^{12}$) is that the model is not capable of giving grid-independent predictions owing to the transition regime along the vertical walls. It was found that the buoyancy source term for the turbulence kinetic energy, G_k, exhibits strong grid sensitivity, as this term is modelled with the Standard Gradient Diffusion Hypothesis (SGDH). By introducing a damping function into this term, the above grid-dependence problem is eliminated and, additionally, the modelled G_k renders correct asymptotic behavior near the vertical wall. The mechanism held in the k-ω model for describing the onset of transition is analyzed. The present approach is simple for practical use and gives reasonable predictions.

Keywords: Turbulent natural convection; Cavity flow; Transition regime; Grid sensitivity; LRN model; k-ω model

Notation

A	aspect ratio for cavity, $A = H/W$
c_μ, c_k, $c_{r\omega}$	model constants
c_1, c_2, c_3	model constants
c_f	wall friction coefficient, $c_f = (H/u_T)(\partial v/\partial x)_w$
E	height of outlet
f_μ, f_k, f_1, f_2	damping functions of turbulence models
h_{in}	height of inlet
H	height of computational domain
k	turbulent kinetic energy
N_{ks}	shear production of k normalized by the dissipation term
N_{kb}	buoyancy production of k normalized by the dissipation term
Nu	local Nusselt number, $-(\partial T/\partial x)_w H/\Delta T$
p	pressure
Pr	Prandtl number, ν/α
Ra	Rayleigh number, $Pr[g\beta(T_h - T_c)H^3/\nu^2]$
R_t	turbulent Reynolds number
T	temperature
T_h, T_c	temperatures at heated and cooled walls, respectively
u_T	velocity scale for cavity flow, $[g\beta(T_h - T_c)H]^{1/2}$
u_i	mean velocity components in the x_i direction
u', v'	fluctuating velocities in the x and y directions, respectively
W	width of computational domain
x_i	Cartesian space coordinates ($i = 1, 2$)

Greek

α	thermal diffusivity
β	thermal expansion coefficient
ΔT	temperature difference, $\Delta T = (T_h - T_c)$
ε	dissipation rate of k
ε_{in}	dissipation rate of k at inlet
μ	dynamic molecular viscosity
μ_t	turbulent dynamic viscosity
ν	kinematic viscosity, μ/ρ
ν_t	turbulent kinematic viscosity, μ_t/ρ
ρ	density of fluid
σ_k, σ_z, σ_T	model constants
τ	turbulent time scale
ω	specific dissipation rate of k
ζ	similarity variable

1. Introduction

Non-isothermal turbulent convection flows are encountered in many engineering applications, including building ventilation, solar energy collectors, cooling of nuclear reactors and material processing. This type of flow is either *buoyancy-affected* or purely *driven* by buoyancy due to thermal stratification. The well-known buoyancy-driven flow is the natural convection in an enclosure with two differentially heated vertical walls, i.e. the so-called "cavity flows".

* Corresponding author. E-mail: lada@tfd.chalmers.se.

0142-727X/99/$ – see front matter
PII: S0142-727X(98)10050-4

Natural convection flows in enclosures usually possess two distinct patterns: the boundary layers along the walls and the encircled recirculating motion in the core. In cases with heated and cooled vertical walls, the laminar air flow at a local Rayleigh number larger than 10^9 may be promoted to turbulent transition in the vertical boundary layer (Incropera and DeWitt, 1990). The transition from laminar to turbulence causes an increase in the convective heat transfer on wall surfaces. In the direct numerical simulations (DNS) for air flow in a square cavity, Paolucci and Chenoweth (1989) detected that, at the critical Rayleigh number between 10^8 and 2×10^8, the flow undergoes a Hopf bifurcation to a periodic unsteady flow. A slightly larger Rayleigh number will make the flow display Tollmien–Schlichting-like waves in the vertical boundary layer. A further increase of the Rayleigh number will lead to the high dimensional turbulent state. Henkes and Le Quéré (1996) revealed numerically that three-dimensional perturbations are less stable than two-dimensional perturbations for air-filled cavity flows and give a lower critical Rayleigh number for transition onset. They also showed that the three-dimensional instability has a combined thermal and hydrodynamic nature.

The transitional flow is essentially of a low-Reynolds/Rayleigh-number type, which is unsteady and not reproducible. It is of practical importance to reasonably predict the onset of transition, for example, in applications of crystal growth and cooling of nuclear reactors. It is well-known, however, that the physical transition phenomenon itself is not tractable with a Reynolds-averaging model, since all the spectra effects are lost in the time-averaging process, and the two-equation models are capable of distinguishing only the magnitude and an average frequency of perturbations that fall in a specific range of frequencies of inducing instability. Nevertheless, the LRN variants of the two-equation models have been widely applied in recent years for simulating transitional flows, particularly for predicting the onset of by-pass transition. A moderate degree of success in such applications has been reported (Savill, 1996).

An important feature of turbulent natural convection flows is that turbulence relies significantly on the thermal stratification. A stable stratification usually dampens turbulence. For natural convection flows in a cavity at moderate Rayleigh numbers, turbulence is fully developed only in some regions along the vertical walls (the upper part along the heated wall and the lower part along the cooled wall), and it decays away from the walls. This thus requires the turbulence models used in the computation to be able to appropriately capture the turbulence evolution starting from laminar state so as to obtain reliable heat transfer predictions. The strong interaction between the thermal and hydrodynamic instabilities requires a particular effort to describe the non-linear growth of disturbances that lead the flow from laminar to turbulence.

Over the past ten years, extensive studies have been made on the buoyancy-driven flows in enclosures through experiments and numerical techniques, because this type of flow is of interest in both fundamental turbulence research and engineering applications. Experimental work, by e.g. Cheesewright et al. (1986) and Giel and Schmidt (1986), has often been used for the validation of numerical computations, which range from DNS, LES and second-moment closures to two-equation eddy viscosity models, see e.g. Paolucci and Chenoweth (1989), Bergstrom and Huang (1997), Davidson (1990a, b) and Henkes et al. (1991) and Heindel et al. (1994). Among the two-equation eddy viscosity models, the k-ε model and its LRN variants have been commonly used. Ince and Launder (1989) introduced the Generalized Gradient Diffusion Hypothesis (GGDH) to model the heat flux vector. Together with the Yap correction in the ε-equation, this approach is able to give satisfactory results. Hanjalic and Vasic (1993) proposed an algebraic heat flux model (AFM), which showed a reasonable behavior. A brief overview of previous work on the computations of turbulent natural convection in two-dimensional enclosures can be found in, e.g., Hanjalic and Vasic (1993). In general, the inclusion of low-Reynolds-number modifications in the k-ε model improves the prediction of wall heat transfer, as stated by Heindel et al. (1994). However, some problems have also been reported in a comparative study using the results from a workshop conducted by Henkes and Hoogendoorn (1995). Among others, the solution was found to be grid-dependent when using the k-ε model with the isotropic eddy diffusivity concept (i.e. SGDH): the transition onset along the non-adiabatic vertical wall is delayed as a result of refining grid, and eventually returning an unrealistic laminar solution.

Wilcox (1994) developed an LRN k-ω model for transition simulation. Unlike the approach usually used for by-pass transition by diffusion of free-stream turbulence into the flow, a method called *numerical roughness strip* was introduced to trigger transition at a specified location. This method is essentially a point transition approach in which the location of transition onset needs to be empirically established. This model was applied to a series of transitional boundary layer flows, and realistic simulations were reported. To improve the predictions for internal low-Reynolds-number recirculating flows, a modified form of this model was proposed by Peng et al. (1997). Both Wilcox's model and the modified model preserve the mechanism for transition simulation of isothermal boundary layer flows as described by Wilcox (1994). For turbulent natural convection flows, however, the behavior of these two models remains unclear. It therefore provides motivation to investigate the performance of these models for flows in which the turbulence is promoted from laminar state by both shear and thermal stratification.

In this work, the two aforementioned LRN k-ω models are used for predicting thermally stratified turbulent flows in enclosures. The influence of thermal stratification on the turbulence evolution is investigated. Emphasis is put on the prediction of transition onset in the boundary layer along the vertical heated/cooled wall. The behavior of the LRN k-ω model is analyzed for predicting transition. By using a damping function for the buoyant source term in the k-equation, together with the simple SGDH approach, the grid-dependence problem for transition prediction is removed, and the grid-independent solution can be asymptotically achieved with successively refined grids. The present approach has been applied to a buoyancy-driven natural convection flow at $\mathrm{Ra} = 5 \times 10^{10}$ in a rectangular cavity and to a mixed convection flow in a square enclosure with unstable thermal stratification. For comparison, two LRN k-ε models by Abe et al. (1994) and by Lam and Bremhorst (1981) are also used. The results have been compared with experimental data.

2. Turbulence models

2.1. Model equations

To describe the evolution of the turbulence field and define the turbulent scales, an equation for turbulence energy is often used when using Reynolds-averaging two-equation models. For steady flows, the transport equation for turbulent kinetic energy, k, is written as

$$\frac{\partial(\rho u_j k)}{\partial x_j} = P_k - \Pi_k + \frac{\partial}{\partial x_j}\left[\left(\mu + \frac{\mu_t}{\sigma_k}\right)\frac{\partial k}{\partial x_j}\right] + S_k, \tag{1}$$

where the right-hand side terms are the production, the dissipation, the diffusion and an additional source term, respectively. In the context of two-equation turbulence modelling, an extra equation is required to construct the eddy viscosity, μ_t. In analogy to the k-equation, this equation is cast into a general form as

$$\frac{\partial(\rho u_j z)}{\partial x_j} = P_z - \Pi_z + \frac{\partial}{\partial x_j}\left[\left(\mu + \frac{\mu_t}{\sigma_z}\right)\frac{\partial z}{\partial x_j}\right] + S_z. \tag{2}$$

The right-hand side of Eq. (2) is termed in a way analogous to those in Eq. (1). In this study, two types of LRN models were used, i.e. the k-ε model and the k-ω model. Eq. (2) then turns out to be a transport equation for ε or ω. The eddy viscosity in the k-ε model is defined as

$$\mu_t = c_\mu f_\mu \frac{\rho k^2}{\varepsilon}. \tag{3}$$

In the k-ω model, it is expressed as

$$\mu_t = c_\mu f_\mu \frac{\rho k}{\omega}. \tag{4}$$

The production term in the k-equation, P_k, is modelled by assuming that the turbulent Reynolds stresses are in alignment with the strain rate tensor, $S_{ij} = (\partial u_i/\partial u_j + \partial u_j/\partial u_i)/2$. This gives

$$P_k = 2\mu_t S_{ij}\frac{\partial u_i}{\partial x_j} = \mu_t\left(\frac{\partial u_i}{\partial x_j} + \frac{\partial u_j}{\partial x_i}\right)\frac{\partial u_i}{\partial x_j}. \tag{5}$$

The two LRN k-ε models used in this work are the Abe–Kondoh–Nagano (AKN) model (1994) and the Lam–Bremhorst (LB) model (1981), and the LRN k-ω models are the Wilcox (WX) model (1994) and a model by Peng, Davidson and Holmberg (PDH) (1997). The terms appearing in Eqs. (1) and (2) are given in Table 1.

The source term in the k-equation, S_k, is due to the buoyancy, which represents the exchange between potential energy and turbulent kinetic energy. This term is associated with the turbulent heat flux in the vertical direction, reading

$$G_k = \rho g \beta \overline{u_j' T'} \delta_{2j}. \tag{6}$$

Several sophisticated options can be used to model this term, e.g. the GGDH model by Ince and Launder (1989) and the AFM approach by Hanjalic and Vasic (1993). For its simplicity, the SGDH model remains most widely used in engineering applications, giving

$$G_k = -g\beta\frac{\mu_t}{\sigma_T}\frac{\partial T}{\partial x_j}\delta_{2j}. \tag{7a}$$

The GGDH model represents the vertical heat flux by including a horizontal temperature gradient in the presence of shear. It reads

$$G_k = -c_\theta g\beta\frac{1}{\omega}\left(2\mu_t S_{2j} - \frac{2}{3}\delta_{2j}\rho k\right)\frac{\partial T}{\partial x_j}. \tag{7b}$$

Depending on the thermal stratification, the buoyant source term in the k-equation either enhances turbulence (as a production term) or dampens turbulence (as a destruction term). For convenience, this term is termed here buoyancy production in cases of both stable and unstable thermal stratification, unless otherwise stated.

An extra term in the PDH model is included in the ω-equation. This term is the turbulent cross-diffusion term (Peng et al., 1997) and is expressed as

$$C_\omega = c_{r\omega}\frac{\mu_t}{k}\frac{\partial k}{\partial x_j}\frac{\partial \omega}{\partial x_j}. \tag{8}$$

The buoyancy source term in the ε- or ω-equation can readily be derived from dimensional analyses, as shown in Table 1. Note that the specific dissipation rate, ω, is a reciprocal of the turbulent time scale, i.e. $\omega \sim 1/\tau$. Eqs. (3) and (4) indicate that $\omega \sim \varepsilon/k$. This suggests that $\mathrm{D}\omega/\mathrm{D}t = (1/k)\mathrm{D}\varepsilon/\mathrm{D}t - (\omega/k)\mathrm{D}k/\mathrm{D}t$. Using this relation, the buoyancy term in the ω-equation can be shown to have the form of $(c_{\varepsilon 3} - 1)(\omega/k)G_k$. In accordance with Rodi's arguments (Rodi, 1984), $c_{\varepsilon 3}$ is close to unity in the vertical boundary layer and close to 0 in the horizontal boundary layer. Henkes et al. (1991) proposed using $c_{\varepsilon 3} = \tanh|v/u|$ to satisfy this argument for computing turbulent cavity flows. Other constant values, ranging from 0.8 to 1.5, have been used for $c_{\varepsilon 3}$ by different researchers, see e.g. Hanjalic and Vasic (1993) and Murakami et al. (1996). Markatos et al. (1982, 1984) stated that there is evidence that the buoyancy effect should be reflected only in the k-equation. Heindel et al. (1994) also detected a negligible effect of constant $c_{\varepsilon 3}$ in the calculations of cavity flows. Based on the relation of $c_{\omega 3} \sim (c_{\varepsilon 3} - 1)$, the effect of $c_{\omega 3}$ was investigated in this work by employing values from -0.3 to 1.0 for cavity flows. Indeed, the prediction appears to be insensitive to this constant. As a consequence, in the present calculations, $c_{\omega 3}$ is set to zero for both the WX and PDH models. The closure constants are summarized in Table 2. The damping functions, f_μ, f_k, f_1 and f_2, for different models are given in Appendix A.

2.2. Transition Regime

At a moderately high Rayleigh number, the natural convection boundary layer flow along a non-adiabatic vertical wall of an enclosure, e.g. the heated wall, usually undergoes three stages: the laminar flow near the lower left corner, and the subsequent transitional and turbulent flows. The transition onset can be observed through the convective heat transfer over the wall surface, in which a sudden jump occurs. The LRN k-ε model, as well as the standard k-ε model, usually predicts a delayed transition regime when refining the grid. Using the standard k-ε model, by triggering transition in the boundary layer with a prescribed amount of kinetic energy, Henkes and Hoogendoorn (1995) found that this grid-dependence problem can be removed. This approach, however, overpredicts the average wall heat transfer. Moreover, introducing prescribed turbulence into a confined system might be unrealistic. Using the LRN k-ω models in this study, delayed transition predictions were also detected by successively refining the grid from 60×60 to 160×160. A possible ex-

Table 1
Terms in turbulence models used in this work

Models	LB model	AKN model	WX model	PDH model
Π_k	$\rho\varepsilon$	$\rho\varepsilon$	$c_k\, f_k\, \rho\, \omega\, k$	$c_k\, f_k\, \rho\, \omega\, k$
S_k	G_k	G_k	G_k	G_k
P_z	$c_1\, f_1(\varepsilon/k)\, P_k$	$c_1\, f_1(\varepsilon/k)\, P_k$	$c_1\, f_1(\omega/k)\, P_k$	$c_1\, f_1(\omega/k)\, P_k$
Π_z	$c_2\, f_2\, \rho\, \varepsilon^2/k$	$c_2\, f_2\, \rho\, \varepsilon^2/k$	$c_2\, \rho\, \omega^2$	$c_2\, \rho\, \omega^2$
S_z	$c_3\, (\varepsilon/k)\, G_k$	$c_3\, (\varepsilon/k)\, G_k$	$c_3\, (\omega/k)\, G_k$	$c_3\, (\omega/k)\, G_k + C_\omega$

Table 2
Model constants

Constants	c_μ	c_k	c_1	c_2	c_3	σ_k	σ_z	σ_T	$c_{r\omega}$
LB model	0.09	–	1.44	1.92	$\tanh\|v/u\|$	1.0	1.3	0.9	–
AKN model	0.09	–	1.50	1.90	$\tanh\|v/u\|$	1.4	1.4	0.9	–
WX model	1.0	0.09	0.56	0.075	0.0	2.0	2.0	0.9	–
PDH model	1.0	0.09	0.42	0.075	0.0	0.8	1.35	0.9	0.75

planation on this uncertainty may be attributed to the mechanism for predicting transition onset preserved in the k-ω model, which is originally subjected to forced convection boundary layer flows.

Comparing to isothermal flows dominated by shear or pressure gradient, buoyancy-driven flows possess one further turbulence evolution mechanism due to thermal stratification as represented by the buoyancy-related term, G_k, in the k-equation. The unknown correlation in G_k reflects the interaction between the fluctuating velocity and temperature fields. If G_k is modelled, say, with the SGDH or the GGDH approach, this term can be written in a general form

$$G_k = g\beta\overline{v'T'} = v_t F\left(\omega, \frac{\partial u_i}{\partial x_j}, \frac{\partial T}{\partial x_j}\right), \tag{9}$$

where F is a function of ω and the gradients of velocities and temperature.

For an incompressible, two-dimensional natural convection boundary layer flow along a vertical heated wall, in analogy to Wilcox's analysis (Wilcox, 1994), the net production per unit dissipation term for k and ω, N_k and N_ω, can be written as, respectively,

$$N_k = \frac{c_\mu f_\mu}{c_k f_k}\left[\left(\frac{\partial v/\partial x}{\omega}\right)^2 + \frac{F}{\omega^2}\right] - 1, \tag{10}$$

$$N_\omega = \frac{c_\mu f_\mu}{c_2}\left[c_1 f_1\left(\frac{\partial v/\partial x}{\omega}\right)^2 + c_3\frac{F}{\omega^2}\right] - 1. \tag{11}$$

Since the ω-equation has a well-behaved solution as $k = 0$, the amplification or reduction of k and ω in magnitude can thus be determined with the sign changes of N_k and N_ω. To ensure transition to occur from laminar to turbulence, k must be amplified earlier than ω (transition will otherwise never occur). It is thus necessary to have $N_k > N_\omega \geqslant 0$. Consequently, this requires, as $R_t \to 0$.

$$\left(\frac{1}{c_k f_k} - \frac{c_1 f_1}{c_2}\right)\left(\frac{\partial v/\partial x}{\omega}\right)^2 + \left(\frac{1}{c_k f_k} - \frac{c_3}{c_2}\right)\frac{F}{\omega^2} > 0. \tag{12}$$

For isothermal boundary layer flows, $F = 0$, Eq. (12) is thus satisfied by simply taking

$$c_1 f_1 c_k f_k < c_2 \quad \text{as} \quad R_t \to 0. \tag{13}$$

Eq. (13) holds true in both the WX model and the PDH model. For natural convection boundary layer flows, this condition is no longer sufficient because the turbulent heat flux contributes to the net productions. As argued above, the model constant c_3 has been set to zero. To trigger transition, the amplification of k depends on both the normalized production due to shear, $N_{ks} = C_{Nk}[(\partial v/\partial x)/\omega]^2$ with $C_{Nk} = c_\mu f_\mu / c_k f_k$, and the normalized production due to buoyancy, $N_{kb} = C_{Nk}F/\omega^2$.

For isothermal boundary layer flows ($F = 0$), Wilcox (1994) showed that N_k and N_ω increase linearly with local Reynolds number along the surface. Through an argument of model constants, k is forced to grow starting from laminar flow at the minimum critical Reynolds number ($\mathrm{Re}_{cr} \approx 9 \times 10^4$) at which the Tollmien–Schlichting waves begin to form in the Blasius boundary layer. For natural convection boundary layer flows along the heated/cooled vertical walls in an enclosure, DNS results by Paolucci and Chenoweth (1989) and by Le Quéré (1992) reveal that Tollmien–Schlichting-like waves occur at a Rayleigh number larger than 2×10^8. This seems to suggest that the free convection boundary layer flow possesses behavior similar to the Blasius boundary layer, of causing transition to turbulence. However, the mechanism held in the k-ω model for transition simulation is quantitatively questionable when $F \neq 0$, as shown in Eqs. (10) and (11). Two uncertain points arise. First, the addition of the buoyancy term in the k-equation could not ensure that k is amplified before ω as $F < 0$ for stable thermal stratification where $\partial T/\partial y > 0$. Second, because the buoyancy term interferes with the net production of turbulence energy, N_k, it cannot guarantee that k starts to grow at the critical Ra number where the secondary instability occurs, e.g. $\mathrm{Ra}_{cr} \approx 2 \times 10^8$ for 2D cavity flows as revealed in DNS. This is essential for accurately predicting the location of transition onset.

The k-ω model has an important feature to enable an analytical observation on the flow change-over from one state to another as transition occurs. That is, the ω-equation uncouples from the k-equation as $k = 0$, giving a nontrivial laminar solution for ω. To further reveal how the transition-onset occurs in response to the model behavior at a certain Rayleigh number, a more comprehensive analysis can be made by a similarity transformation of Eqs. (10) and (11). It should be noted that the analysis is started from laminar state and ended up with the change-over of the flow state where the local production of k sufficiently overwhelms its local dissipation and transition occurs.

According to Henkes (1990), the quantities H, $\Delta T = (T_h - T_{ref})$ and $u_T = (g\beta\Delta T H)^{1/2}$ are appropriate scalings for y, T and v, respectively. Here, T_{ref} is a reference temperature (e.g. $T_{ref} = T_c$ for cavity flow). Further, a similarity variable, ζ, is used for the following transformation of Eqs. (10) and (11) (White, 1974; Cebeci and Khattab, 1975) and

$$\zeta = \left(\frac{u_T^2}{4\nu^2 H y}\right)^{1/4} x. \tag{14}$$

Note that x is normal to the vertical wall, and y is the streamwise direction along the wall. With this similarity variable and the above scalings, v and T are then written in terms of ζ, i.e.

$$v = u_T V(\zeta), \tag{15}$$

$$T = \Delta T \Theta(\zeta). \tag{16}$$

By means of the asymptotic solution of ω, $\omega \propto 1/x^2$ as $x \to 0$, ω can be expressed as

$$\omega = \left(\frac{u_T^2}{4Hy}\right)^{1/2} \Omega(\zeta). \tag{17}$$

The SGDH approach in Eq. (7a), which gives $F = -(g\beta/\sigma T) \times (\partial T/\partial y)$, is used to model the buoyancy term G_k. Setting $c_3 = 0$ and using Eqs. (14)–(17) in Eqs. (10) and (11) yield, respectively,

$$N_k = \frac{c_\mu f_\mu}{c_k f_k}\left[2\left(\frac{\mathrm{Ra}}{\mathrm{Pr}}\right)^{1/2}\left(\frac{y}{H}\right)^{1/2}\left(\frac{\partial V/\partial\zeta}{\Omega}\right)^2 + \left(\frac{\zeta}{\sigma_T}\right)\left(\frac{\partial\Theta/\partial\zeta}{\Omega^2}\right)\right] - 1, \tag{18}$$

$$N_\omega = \frac{c_\mu f_\mu c_1 f_1}{c_2}\left[2\left(\frac{\mathrm{Ra}}{\mathrm{Pr}}\right)^{1/2}\left(\frac{y}{H}\right)^{1/2}\left(\frac{\partial V/\partial\zeta}{\Omega}\right)^2\right] - 1. \tag{19}$$

A dramatic amplification in k (starts as N_k changes its sign to positive) indicates the onset of transition, whereafter the amplification of ω controls the width of transition. Note that the turbulence energy starts to grow as the first term in Eq. (18) reaches unity. Somewhere after this point, the eddy viscosity suddenly increases and the transition from laminar to turbulence occurs. At the onset position of transition, this suggests

$$\lambda_1\left(\frac{\mathrm{Ra}}{\mathrm{Pr}}\right)^{1/2}\left(\frac{y}{H}\right)_{\mathrm{tr}}^{1/2} + \lambda_2 = \alpha_0 \quad (\alpha_0 > 1), \tag{20}$$

where

$$\lambda_1 = \frac{2c_\mu f_\mu}{c_k f_k}\left(\frac{\partial V/\partial\zeta}{\Omega}\right)^2, \qquad \lambda_2 = \frac{c_\mu f_\mu}{c_k f_k \sigma_T}\left(\frac{\zeta\partial\Theta/\partial\zeta}{\Omega^2}\right). \tag{21}$$

In Eqs. (20) and (21), λ_1 and λ_2 are functions of the similarity variable, ζ. As the transition occurs, the position (height) of transition onset, y_{tr}, can thus be estimated by solving Eq. (20) for $(y/H)_{\mathrm{tr}}$. This gives

$$y_{\mathrm{tr}} = \left(\frac{\mathrm{Pr}}{\mathrm{Ra}}\right)\left(\frac{\alpha_0 - \lambda_2}{\lambda_1}\right)^2 H. \tag{22}$$

Note that $\alpha_0 = (N_{ks} + N_{kb})_{\max}$ is the maximum total production per unit dissipation as transition occurs. Eq. (22) shows that the height of laminar-turbulent transition along a vertical heated wall decreases with an increasing Rayleigh number. For buoyant flows in a square cavity, Henkes (1990) used Chien's LRN k-ε model (Chien, 1982) to numerically reveal the dependence of y_{tr} on Ra. It was shown that y_{tr} tended to be zero as the Rayleigh number was up to 10^{17}. Eq. (22) suggests that an appropriate prediction of y_{tr} depends on the model behavior of simulating λ_1, λ_2 and α_0 when the flow approaches transitional state from laminar. Usually, λ_1 reaches its maximum value somewhere near the velocity peak in the boundary layer, where $|\lambda_2|$ is often rather small due to near-wall large ω, having $|\lambda_2| \ll 1 < \alpha_0$.

To ensure the occurrence of transition, two essential conditions should be emphasized. First, the net production N_ω should not reach zero earlier than N_k. Second, the value of α_0 should be raised to a certain level in the boundary layer. With unstable thermal stratification, the buoyant source term in the k-equation usually contributes to the enhancement of the level of α_0. For stable thermal stratification, by contrast, this term is often negative as modelled with the SGDH. To raise α_0 to be a positive value and much larger than unity, it thus relies solely on the shear production, whose maximum value often arises in the near-wall boundary layer whereas the buoyancy production is usually negligibly small (Davidson, 1992). This, however, by no means suggests a negligible role played by the buoyancy-related term. In the neighboring outer region of the boundary layer this term can be relatively high with negative values, behaving as a energy destruction term. In contrast to the by-pass transition where the freestream turbulence is diffused into the boundary layer, in this case the turbulence energy generated by shear in the boundary layer may be *diverged* to the outer region in which the energy destruction is reinforced by the buoyant source term. Such a modelling feature may deter α_0 from reaching a desired level to trigger transition. The model will consequently predict a delayed transition or even an unrealistic laminar solution. Special care must then be taken of the buoyant source term in the outer region neighboring to the boundary layer.

Indeed, there is evidence that the aforementioned grid-dependence of the transition prediction is related to the buoyancy-generated source. This can be verified by dropping the buoyancy term in the k-equation. It was found that this exclusion can rid the model of the grid-dependent behavior, but the heat transfer is largely over-predicted as compared with experiments and the turbulence energy in the core region is not sufficiently dampened as desired. This implies that a simple exclusion of G_k is not acceptable. Since the buoyant source term tends to suppress turbulence in stable thermal stratification, an inclusion of this term is thus preferable. On the other hand, G_k must then be appropriately modelled, because the amplification of the local k production in the near-wall boundary layer is associated with this term. If the turbulence in the neighboring outer region is over-suppressed (through G_k with negative sign), the amplification of the near-wall shear production may be slowed down by diffusion of turbulence energy towards the outer region so as to compensate for the stabilization there. This will consequently delay the transition onset, or even cannot sustain the turbulence evolution in the boundary layer, and retaining the flow in laminar state.

To remove this undesired behavior induced due to thermal stratification, measures must be taken to control the performance of the buoyant source term, G_k. It should be noted that more sophisticated models, e.g., the GGDH model (Ince and Launder, 1989) and the AFM approach (Hanjalic and Vasic, 1993), can be used to approximate this term. These two models were applied in the original work to the same cavity flow as considered in this work. There was no grid-dependence problem reported as such identified here when using LRN two-equation models together with the SGDH approach. The rationale now seems clear: models that approximate G_k in such a way that the normalized production (and thus α_0) in the boundary layer keeps growing can remove the above problem and lead the flow from laminar to turbulence. Indeed, Davidson (1992) showed that G_k is even positive in the outer region when using the GGDH model while it is negligibly small in the near-wall region comparing to other terms. Using the AFM, Hanjalic and Vasic (1993) stated that G_k is usually less than one-third of the shear production in the outer layer. This implies that the shear production itself in the outer layer has the capability to compensate for the energy destruction without extra turbulence diffusion from the inner region. We believe that such modelling features inherent in the GGDH and AFM approaches may, to some extent, bring about the success in avoiding the grid-dependence problem as in the present consideration. Although these two approaches are not included in the following computations, it can be shown that the predictions given by the present simple approach are actually very similar to the results produced by the GGDH and AFM methods.

Since the grid-dependence problem is encountered when using the SGDH, which has so far gained the greatest popularity in practical applications for its simplicity, the SGDH model is thus the main consideration to overcome the problem inherent in this approach. For this purpose, a practical way is to use a damping function that is able to appropriately deter

the buoyant source term in the outer region from absorbing too much energy powered by the near-wall shear production. Furthermore, the method of using a damping function for G_k is supported by an asymptotic analysis near the vertical wall: using the SGDH approach, Eq. (7a), gives rise to an incorrect asymptotic behavior for the modelled G_k. Near the vertical wall, $v' \propto x$, $T' \propto x$ (cf. So and Sommer, 1994). The exact buoyancy source term is thus proportional to x^2 as $x \to 0$. Since $\mu_t \propto x^3$ for the PDH model, and $\mu_t \propto x^4$ for the WX model, with $\partial T/\partial y \propto x^0$ as $x \to 0$, the modelled G_k term then has a relation of $G_k \propto x^3$ for the former and of $G_k \propto x^4$ for the latter. Note that the GGDH approach also renders incorrect asymptotic behavior near the vertical wall.

The devised damping function, f_G, is employed in the PDH model, having $f_G \propto 1/x$ as $x \to 0$. Note that the use of a damping function will give an incorrect asymptotic behavior for G_k near a horizontal wall (for models with $\mu_t \propto y^3$), where $v' \propto y^2$ as $y \to 0$, but this is of no significant consequence since the flow along the vertical walls is dominant in an overall fashion for flows induced by heated/cooled vertical walls. The role played by the damping function is mainly to constrain the turbulence destruction due to buoyancy and thus to suppress the turbulence energy diffusion from the boundary layer to the neighboring outer region so as to avoid delayed prediction of transition onset as analyzed above, and additionally, to obtain correct asymptotic behavior for G_k near the vertical wall. This function was devised as

$$f_G = \left\{1 - \exp\left[-\left(\frac{R_t}{c_g}\right)^3\right]\right\} \times \left(1 + \frac{10}{R_t^{3.25}}\right), \tag{23}$$

where $c_g = 12$, which is numerically optimized. By using this damping function together with the PDH model (hereafter PDH+D), as shown in the next section, the grid-dependence problem can be eliminated. The buoyancy source term in the k-equation is thus modelled as

$$G_k = -g\beta f_G \frac{\mu_t}{\sigma_T}\frac{\partial T}{\partial x_j}\delta_{2j}. \tag{24}$$

The buoyancy production (normalized by the dissipation term), N_{kb}, is often rather small in the boundary layer. The transition onset from laminar to turbulence therefore relies strongly on the shear production (through α_0 and λ_1).

It should be pointed out that the above analysis can also be expected to be applicable for the WX model and for LRN k-ε models by transforming the ε-equation into an ω-equation with the relation of $\varepsilon \sim k\omega$ (see Peng, 1998). The proposed approach is applied, however, only to the PDH model in this study for verification.

3. Solution procedure

The above LRN models have been applied to two non-isothermal convection flows: the turbulent buoyancy-driven flow in a rectangular cavity with $A = 5$, for which the experiment was made by Cheesewright et al. (1986); and the turbulent mixed convection flow in a square enclosure with a heated bottom wall, as in the Blay et al. experiment (Blay et al., 1992).

All the computations have been performed on the basis of the Boussinesq assumption. The air properties are evaluated at a reference temperature: the density is calculated from the gas law, and the dynamic viscosity is calculated by using the Sutherland formula.

The finite volume method is used to discretize the partial differential equations on a collocated grid (Davidson and Farhanieh, 1992). The QUICK scheme is employed for the convection terms in the momentum equations and in the thermal energy equation, and the convection term in the turbulence transport equations is discretized by using the hybrid upwind-central scheme. In order to verify that the low numerical accuracy in the turbulence-convection discretization has not contaminated the prediction of transition, a second-order accurate bounded scheme by van Leer (van Leer, 1974) was also employed to discretize the turbulence-convection term. The resulting predictions, however, were found to be nearly identical to those obtained with the hybrid scheme, and the model eventually renders a laminar solution with refining grid for the cavity flow when not using the damping function in G_k. This seems to imply that the grid-dependence problem in the present transition prediction is not rooted in the numerical accuracy of the turbulence-convection scheme.

To account for the velocity-pressure coupling, the SIMPLEC algorithm is applied. The resulting algebraic equations for velocity components and turbulence quantities are solved iteratively with a line-by-line TDMA solution procedure, and the Strongly Implicit Procedure (SIP) is used to solve the pressure-correction equation. Steady state solution is obtained by using under-relaxation technique and a false time step to ensure a stable solution procedure.

The use of LRN models requires a sufficient number of grid points in the near-wall boundary layer. Special attention has thus been paid to the grid refinement, particularly for computing the buoyancy-driven cavity flow. Non-uniform grid has been used in all the calculations, with the grid clustered in the near-wall region to resolve the wall-damping effect.

The low-Reynolds-number modifications allow the turbulence model to be integrated directly towards the wall surface, without using wall functions as a bridge. On the wall surface, the boundary values for u, v and k were set to zero, while the temperature, as well as the inlet conditions in the mixed convection case, was specified in accordance with experiments.

Neumann boundary conditions were used for all the variables at the outlet. With both the LB and the AKN k-ε models, the wall condition for ε was specified as

$$\varepsilon_w = 2\nu\left(\frac{\partial\sqrt{k}}{\partial n}\right)_w^2. \tag{25}$$

This relation was derived from a balance of the k-equation in the viscous sublayer by using a Taylor series expansion (To and Humphrey, 1986). By means of a similar balance for the ω-equation, an asymptotic expression for ω as the wall is approached can be obtained (Wilcox, 1994)

$$\omega = \frac{6\nu}{c_2 y^2} \quad \text{as} \quad y \to 0. \tag{26}$$

Eq. (26) is employed for calculating ω at the first grid point close to the wall surface.

4. Results and discussion

The results computed with various turbulence models are presented in this section, and are discussed through comparison with experimental data.

4.1. Natural convection in a rectangular cavity

Various cavity configurations have been used in previous experimental and numerical work. Henkes and Hoogendoorn (1995) proposed in a Eurotherm Workshop the use of a square enclosure as the benchmark test case. In their comparison study using the workshop results, they showed that the results for cavities with aspect ratios of 1 and 5 (at nearly the same Rayleigh number) are very close only if they are scaled by the

cavity height. Hanjalic and Vasic (1993) found that the prediction is more erroneous for the flow in a tall cavity with an LRN k-ε model than for the flow in a square or lower-aspect ratio cavity with the same LRN model. For a direct comparison with experimental data, the flow in a rectangular enclosure with an aspect ratio of $A = 5$ was computed. The Rayleigh number is about 5×10^{10} with $T_h = 77.2$ and $T_c = 31.4$. The horizontal walls are assumed to be adiabatic.

When using the LRN k-ε model, the computation needs to be started with some initial turbulence. It was found that the LB model and the AKN model may give a laminar solution with both 60×60 and 80×80 grids unless the initial values of k and ε are specified in such a way that the initial eddy viscosity is about 100 times higher than the molecular one. This was also observed by Hanjalic and Vasic in their previous computations (Hanjalic, Private communication, 1997). However, such an initial specification does not lead to a turbulent solution when using a finer grid, e.g. 160×160, at which the model always eventually returns a laminar solution even though a rather high initial value was given to k. With a grid of 120×120, the AKN model was observed to first give turbulent solution, but this solution did not sustain as further iterations were performed. This phenomenon may be attributed to the non-uniqueness of the transition, as explained by Henkes et al. (1991), the model has a bifurcation point at Ra_{cr}.

With the LRN k-ω models, a very small initial value, e.g. 10^{-10}, was specified for both k and ω. This initial specification is able to give a turbulent solution with a grid refined to, e.g., 120×120. Note that this in fact implicitly sets a rather high initial turbulent Reynolds number, $R_t = k/\nu\omega$. It was found that the WX model and the PDH model also rendered a laminar solution if a small initial turbulent Reynolds number was set by specifying either a smaller initial value of k or a larger ω. Using both the WX and PDH models, we also tried to start the computation with a laminar solution for u, v and ω with a very small initial k value (e.g. 10^{-10}), but the solution remained in laminar stage. This laminar solution was kept even when a numerical roughness strip, as proposed by Wilcox (1994) to trigger transition in forced convection boundary layer flows, was specified around the transition regime. This seems to indicate that the numerical-roughness-strip approach does not work for the present case.

It is desired to attain an asymptotically grid-independent solution by means of refining grid. The grid used in this study was successively refined from 60×60, 80×80, 100×100, 120×120, 160×160 to 180×180. All the models turn out to be strongly sensitive to grid refinement.

Fig. 1 shows that the predicted onset of transition along the vertical wall is delayed with refined grids. As with the LRN k-ε model, the two LRN k-ω models also give grid-dependent predictions, see Fig. 1(c) and (d), although the delay is relatively slow. By refining the grid further, it can be expected that these two models will finally return a laminar solution, as the LRN k-ε model does. The shift of transition with refining grids suggests a delayed amplification of local turbulence production, though this amplification has occurred before dissipation is amplified (on a coarser grid). Refining the grid seems to increase the amplification rate for the dissipation and eventually, the amplification of local turbulence production may be overwhelmed by the local dissipation. Moreover, it was found that all the models used here give reasonable k-distributions (not shown here) as compared with the experimental data provided that they predict the transition onset at $y_{tr}/H = 0.3$ – 0.4 (along the hot wall) with a certain grid. However, this position does not agree with the experimental result. Bowles and Cheesewright's experiment (Bowles and Cheesewright, 1989) gave $y_{tr}/H \approx 0.22$. An earlier transition ($y_{tr}/H < 0.3$) predicted by a model corresponds in general to a lower prediction of the k-peak downstream of the transition regime in the boundary layer. The contradiction between the prediction

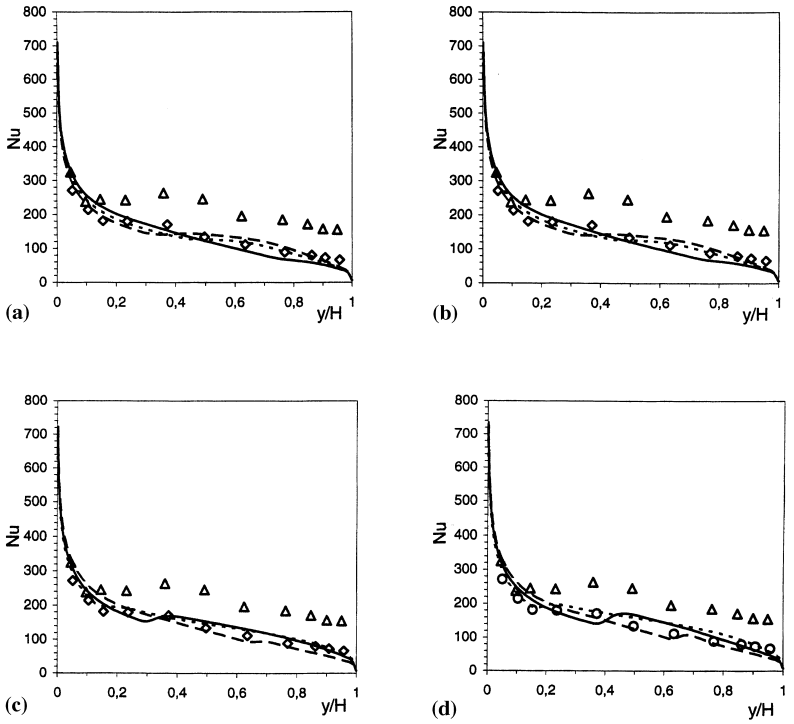

Fig. 1. Grid-dependence of the solution: Nusselt number, Nu, along the vertical wall. (– – –) Grid 60×60, (· · · · · · · · ·) Grid 80×80, (——) Grid 120×120, (- · - · -) Grid 160×160, (Δ) Experiment (hot wall), (◇) Experiment (cold wall). (a) AKN model, (b) LB model, (c) WX model, (d) PDH model.

and the experiment may possibly be due to the heat loss through the horizontal walls in the experiment, as stated by Cheesewright et al. (1986). The heat loss may have affected the measured position of transition onset along the vertical wall.

When using the PDH + D model, the computed convective heat transfer along the heated vertical wall is given in Fig. 2(a), and the k-distribution at the mid-section ($y = H/2$) is shown in Fig. 2(b). By refining the grid successively from 80×80 to 180×180, an asymptotically grid-independent solution is achieved. This indicates that the use of a damping function, f_G, in G_k does prevent the model from being grid-dependent in transition prediction. Again, the lower k-peak is related to the predicted location of transition regime, which is however in reasonable agreement with the prediction using the AFM approach by Hanjalic and Vasic (1993). When using the PDH+D model, all the results shown below were obtained with a grid of 160×160, where the solution can be regarded as being grid-independent, as disclosed in Fig. 2.

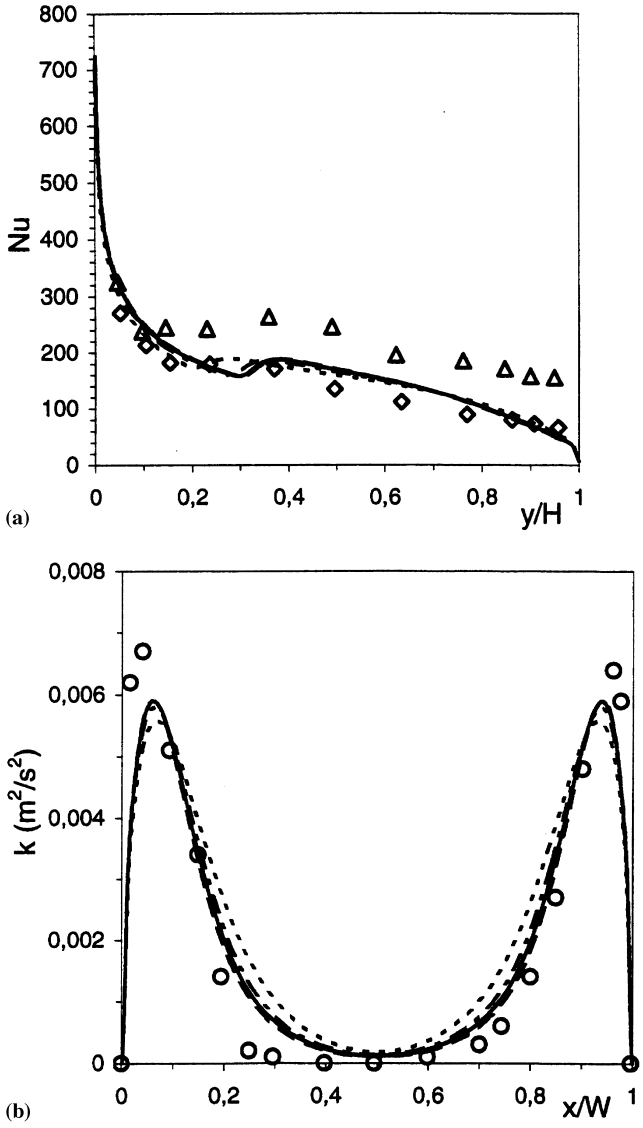

Fig. 2. Predictions using the PDH + D model with refined grids. (· · · · · · · · ·) Grid 80×80, (- · - · -) Grid 120×120, (——) Grid 160×160, (– – –) Grid 180×180. (a) Nusselt number, Nu, along the vertical wall. (b) Turbulence kinetic energy, k, at section $y = H/2$.

Fig. 3(a)–(c) gives the distributions, computed with the PDH+D model, for the mean velocity, temperature and turbulent shear stress at $y = H/2$. Also shown in Fig. 3(d) is the friction coefficient along the vertical walls. As seen, the results are in satisfactory agreement with the experimental data.

The influence of the constant c_g in the damping function f_G was also investigated. It was found that the prediction of transition onset is rather sensitive to the value of f_G. A smaller c_g, i.e. a larger f_G, makes the model predict a later transition. This observation confirms the above analysis that the buoyant source term, as modelled with the SGDH, tends to slow down the turbulence evolution in the boundary layer and delay the transition onset.

To investigate the different roles played by the shear production and the buoyancy production in the k-equation, it is desirable to compare their respective contribution to the turbulence evolution in the boundary layer as transition occurs. The budget for the k-equation in the PDH + D model is given in Fig. 4 at location $y = 0.3H$, which corresponds to the predicted onset position of the transition regime along the heated wall. The k-budget at $y = H/2$ was also investigated (not shown here), indicating that the balance of the k-equation in the boundary layer downstream of the transition regime is sustained mainly by the shear production, the dissipation and the diffusion. Moving to the location of transition onset (at $y = 0.3H$), as shown in Fig. 4, the convection term becomes also significant in the balance, because the turbulence energy grows rapidly as approaching to this stage. In the outer region away from the boundary layer, all the terms become so small that it is difficult to distinguish their separate functions in triggering transition at the post-laminar stage.

As argued above, one of the essential conditions to trigger laminar-turbulent transition is that the total production per unit dissipation term for k due to shear and buoyancy, i.e. $(N_{ks} + N_{kb})$, must grow over unity before transition occurs. Moreover, the turbulent kinetic energy must be amplified earlier than its dissipation. Instead of using the direct budget comparison, a reasonable way is then to compare the dissipation-term-normalized productions, N_{ks} and N_{kb}, near the position where transition occurs. In Fig. 5(a) and (b), such a comparison is made for the PDH model. Because this model is sensitive to the grid density, the distributions obtained with two grids, 120×120 and 160×160, are used to observe the influence of refining grid. With a 120×120 grid, the model predicts a transition onset at $y \approx 0.38H$ and gives reasonable predictions for the other variables. At this grid level, the normalized production due to shear, N_{ks}, grows in the near-wall layer up to a maximum value of about 5.2 (at $x/W = 0.0164$, $\zeta = 1.54$), whereas N_{kb} is about -0.00175. This gives $\alpha_0 = (N_{ks} + N_{kb})_{\max} \approx 5.2$ as transition starts. In the neighboring outer region, by contrast, N_{kb} is negatively dominant over N_{ks} and its absolute value is much larger than the maximum N_{ks} in the near-wall layer. If the maximum numerical value of λ_1 in the boundary layer ($\approx 3.2 \times 10^{-5}$) and the corresponding value of λ_2 there ($\approx -1.75 \times 10^{-3}$) are used in Eq. (22), it gives $y_{tr} \approx 0.38H$ (Pr = 0.72 for air). This is identical with the predicted location of transition onset. When the grid is refined to 160×160, the normalized production, N_{kb}, at the position $y \approx 0.38H$, where the transition occurs for a 120×120 grid, decreases rapidly to large negative values in the outer region, and N_{ks} is brought down with a maximum value of about 1.9 in the inner layer at $x/W = 0.0325$, see Fig. 5(a). Note that no transition occurs at this position with a 160×160 grid. Instead, the predicted transition shifts to $y_{tr} \approx 0.63H$ with this grid, as shown in Fig. 1(d). The result in Fig. 5 suggests that a finer grid may over-amplify the buoyant source term in the neighboring outer region and bring down the shear

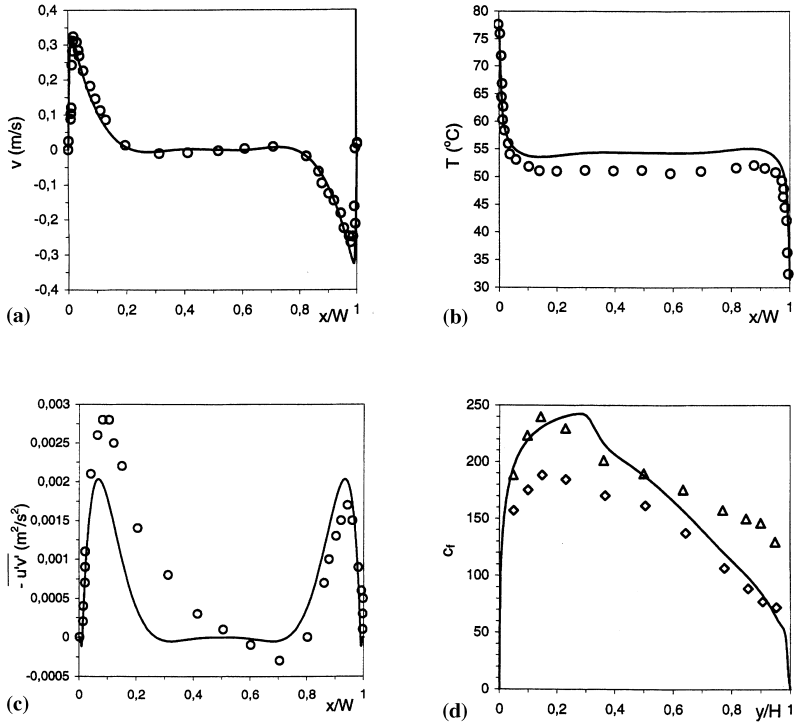

Fig. 3. Predictions using the PDH+D model. The line is for the prediction and the symbols for the experimental data. (Δ) Hot wall, (◇) Cold wall.

production in the boundary layer. As a result, the transition onset is delayed.

On the one hand, the turbulence growth in the boundary layer relies solely on the shear production. The use of damping function f_μ will in general delay the transition onset, as shown by Eqs. (21) and (22) where $|\lambda_2| \ll 1$ near the vertical wall. On the other hand, the turbulence energy is diffused from the near-wall layer to the neighboring outer region, and is "absorbed" owing to the stable thermal stratification and the stabilization function of the horizontal boundary layers. An appropriate equilibrium between the near-wall production amplification and the outer-region energy destruction is thus needed to make the model reasonably represent the transition onset. The result in Fig. 5 indicates that the SGDH as used in the PDH model has over-amplified the buoyant source term, G_k, in the neighboring outer region before transition occurs. This over-estimation is so large (negatively) that the capability of the shear production in the boundary layer is not large enough as a resource to diffuse energy towards the outer region in order to balance the energy destruction there (due to mainly the buoyancy-related term and partly the dissipation term). This is reflected by the fact that the normalized buoyant production in the outer region (with negative value) is much larger than the normalized shear production in the boundary layer (with positive value). Since the energy destruction in the outer region cannot be "saturated" by diffusion of turbulence energy from the near-wall layer, the turbulence evolution in the boundary layer will not go further. Consequently, the value of α_0 in Eq. (22) is deterred from growing to a certain level to trigger transition at a desired location. It is interesting to note that the over-amplification of G_k is reinforced for refining grid. The finer the grid is, the more is the over-estimation of G_k and thus the more the shear production is reduced. With a sufficiently refined grid, the shear production in the near-wall boundary layer is reduced to a level at which the amplification rate of turbulence energy becomes slower than that of the dissipation rate. The near-wall shear production is eventually not able to sustain a continuous amplification of k so as to bring a change-over of the flow state. By contrast, the amplification of dissipation is continued. As long as the local dissipation overwhelms the local production, the k-equation goes to a new balance with a very large ω and a very small k. The model eventually returns a laminar solution, and no transition will arise at all.

In Fig. 6(a) and (b), the normalized productions are compared for the PDH+D model at the transition onset location

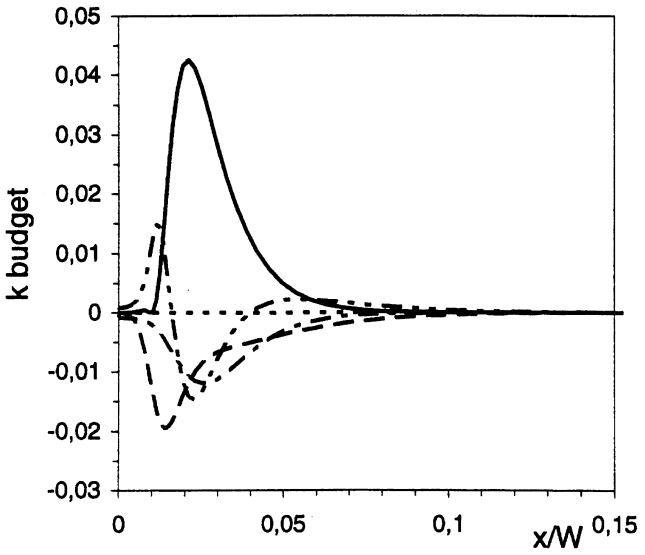

Fig. 4. Contributions of different terms in the k-equation for the PDH+D model at $y = 0.3H$. (– – –) Convection, (——) Shear production, (· · · · · · · · ·) Buoyancy production, (- · - · -) Dissipation, (- · · -) Diffusion.

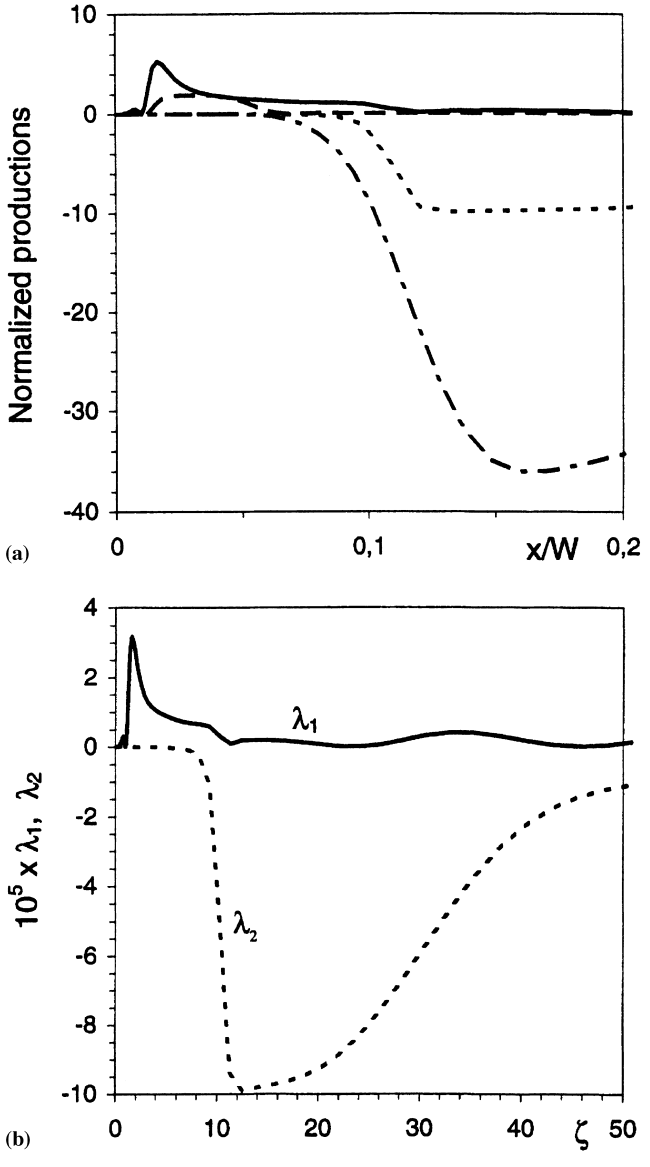

Fig. 5. Near-vertical-wall normalized productions for the PDH model at predicted transition onset location for 120×120 grid ($y_{tr} \approx 0.38H$). (a) Grid-dependence of N_{ks} and N_{kb} at $y = 0.38H$. (——) N_{ks} (120×120), (· · · · · · · · ·) N_{kb} (120×120), (– – –) N_{ks} (160×160), (- · · · -) N_{kb} (160×160). (b) Numerical values for λ_1 and λ_2 at $y = 0.38H$ with a 120×120 grid.

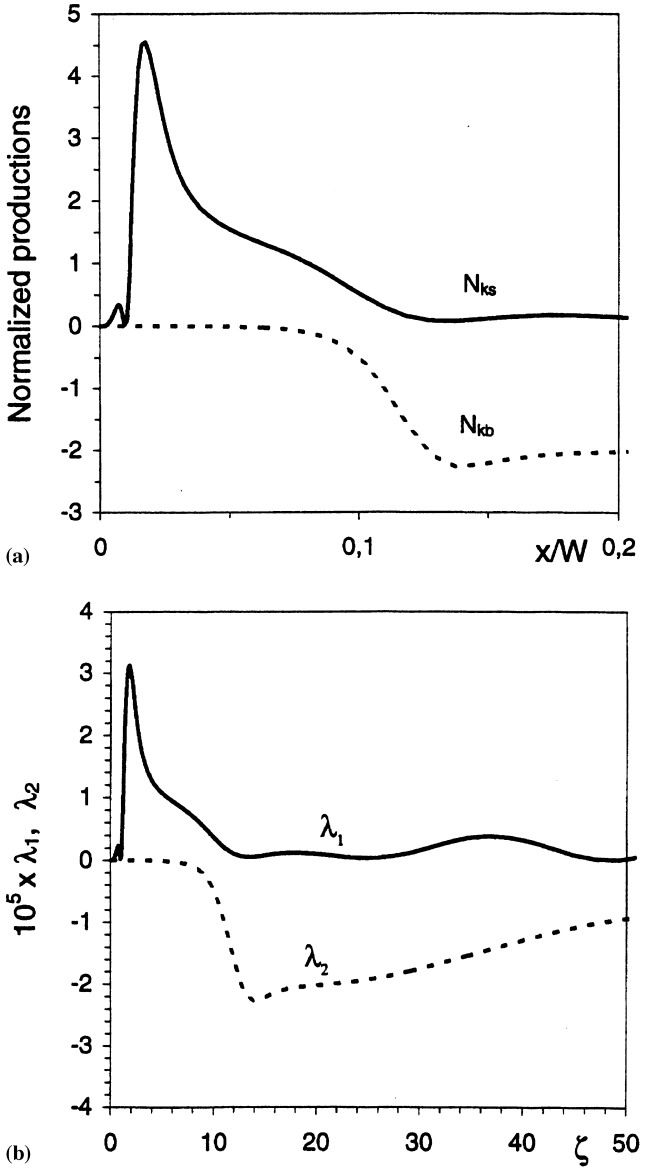

Fig. 6. Near-vertical-wall normalized productions for the PDH + D model at predicted transition onset location ($y_{tr} \approx 0.3H$). (a) Distributions of N_{ks} and N_{kb} at $y = 0.3H$. (b) Numerical values for λ_1 and λ_2 at $y = 0.3H$.

($y_{tr} \approx 0.3H$) predicted by this model on a 160×160 grid. Note that this location is a grid-independent prediction. Fig. 6(a) shows that $|N_{kb}|$ is significantly reduced in the neighboring outer region of the boundary layer by means of the damping function. The maximum normalized shear production occurs at $x/W \approx 0.0177$ ($\zeta \approx 1.77$) with $(N_{ks})_{max} = 4.55$, whereas $N_{kb} = -2.02 \times 10^{-4}$. This gives $\alpha_0 \approx 4.55$, where the numerical value for λ_1 is found to be 3.12×10^{-5} and $\lambda_2 = -2.02 \times 10^{-4}$, see Fig. 6(b). Eq. (22) thus gives $y_{tr} \approx 0.3H$ as does the model.

Unlike with the PDH model, the value of $|N_{kb}|_{max}$ in the outer region becomes smaller than $(N_{ks})_{max}$ in the near-wall boundary layer with the PDH+D model. This implies that the shear production has an extra capability to enhance turbulence in the boundary layer besides to diffuse energy towards the neighboring outer region so as to saturate the turbulence destruction there. The results in Fig. 6 indicate that a reasonable approximation for the buoyant source term can be achieved if the normalized buoyancy production in the outer region is suppressed below the normalized shear production in the near-wall boundary layer. Under this condition, the model becomes insensitive to the grid refinement in predicting transition onset, whose location depends now on the degree of damping of the buoyancy term. A strong damping of this term means that a large extra capability retains in the near-wall shear production to enhance turbulence in the boundary layer, and thus triggering an earlier transition, and vice versa. This is consistent with the previous analysis.

For a natural *laminar* convection boundary layer flow along a vertical flat plate, λ_1 is a similarity parameter whose streamwise dependence vanishes. Assuming there exists a near-wall streamwise-independent maximum value for λ_1 next to the transition regime in the upstream laminar stage where $|\lambda_2|$ is usually much smaller than α_0, a condition for the total

normalized production α_0 to trigger transition at the desired location (y_{tr}/H) is then

$$\alpha_0 = (N_{ks} + N_{kb})_{max} \approx \left(\frac{Ra}{Pr}\frac{y_{tr}}{H}\right)^{1/2}\lambda_1. \quad (27)$$

Eq. (27) appears to be a necessary condition for a two-equation LRN model to correctly predict the onset location of transition regime in the natural convection boundary layer flow along a vertical heated/cooled wall.

4.2. Mixed convection in a square cavity

For the cavity flow with stable thermal stratification, the foregoing computation showed that the SGDH performs reasonably well in conjunction with a damping function by which the grid-dependence problem inherent in this approach is removed for transition prediction in the boundary layer. The present proposal is essentially motivated for dealing with natural convection flows, in which transitional boundary layers exist and cause problems in numerical simulations. This, however, should not constrain its relevance to other internal turbulent buoyant flows.

To further verify the performance of the model for other thermally stratified flows, a mixed convection flow is considered in this subsection. The prediction was compared with the experimental data by Blay et al. (1992). In this case, the air flow is induced into a square cavity ($H \times W = 1.04$ m $\times$ 1.04 m) through a slot ($h_{in} = 0.018$ m) under the top wall and exhausted through an opening ($E = 0.024$ m) on the opposite side above the bottom wall. The supplied air has the same temperature as that on the surfaces of the side and top walls, $T_{in} = T_w = 15$°C. The bottom wall was heated to a constant surface temperature of 35.5°C. Unlike in the closed cavity flow, an unstable thermal stratification is set up near the horizontal walls in this case. The supply conditions at the inlet are: $u_{in} = 0.57$ m/s, $v_{in} = 0$ and $k_{in} = 0.00125$ (m/s)^2 (Blay et al., 1992). The dissipation rate of k is given by $\varepsilon_{in} = c_\mu k_{in}^{3/2}/(0.5\, h_{in})$. The inlet ω value is estimated by using the relation of $\omega \sim \varepsilon/k$. A 100 × 100 non-uniform grid was used to perform the computation.

Fig. 7 shows the results comparing with the experimental data at the vertical and horizontal mid-sections (at $y = H/2$ and $x = W/2$, respectively). The LRN k-ε models used in this work generally give less satisfactory predictions than the LRN k-ω models do. The mean velocity is over-predicted by the AKN model, and the LB model over-estimates both the temperature and the turbulence energy. None of the LRN k-ε models gives overall reasonable predictions for the turbulent kinetic energy. All the models over-predict the mean velocity near the wall, with the result from the PDH model closest to the experiments. The PDH model produces satisfactory predictions for k in near-wall regions. The turbulence energy in the recirculating region predicted by the WX model agrees well with the experimental data, although this model significantly under-predicts the near-wall k level.

As shown in Fig. 7, introducing the damping function f_G into the PDH model (the PDH+D model) produces nearly same distributions for the mean quantities as the PDH model does. The turbulent kinetic energy is, however, slightly over-estimated in the near-wall region. In general, the prediction obtained with the PDH+D model is satisfactory and very similar to that computed with the PDH model.

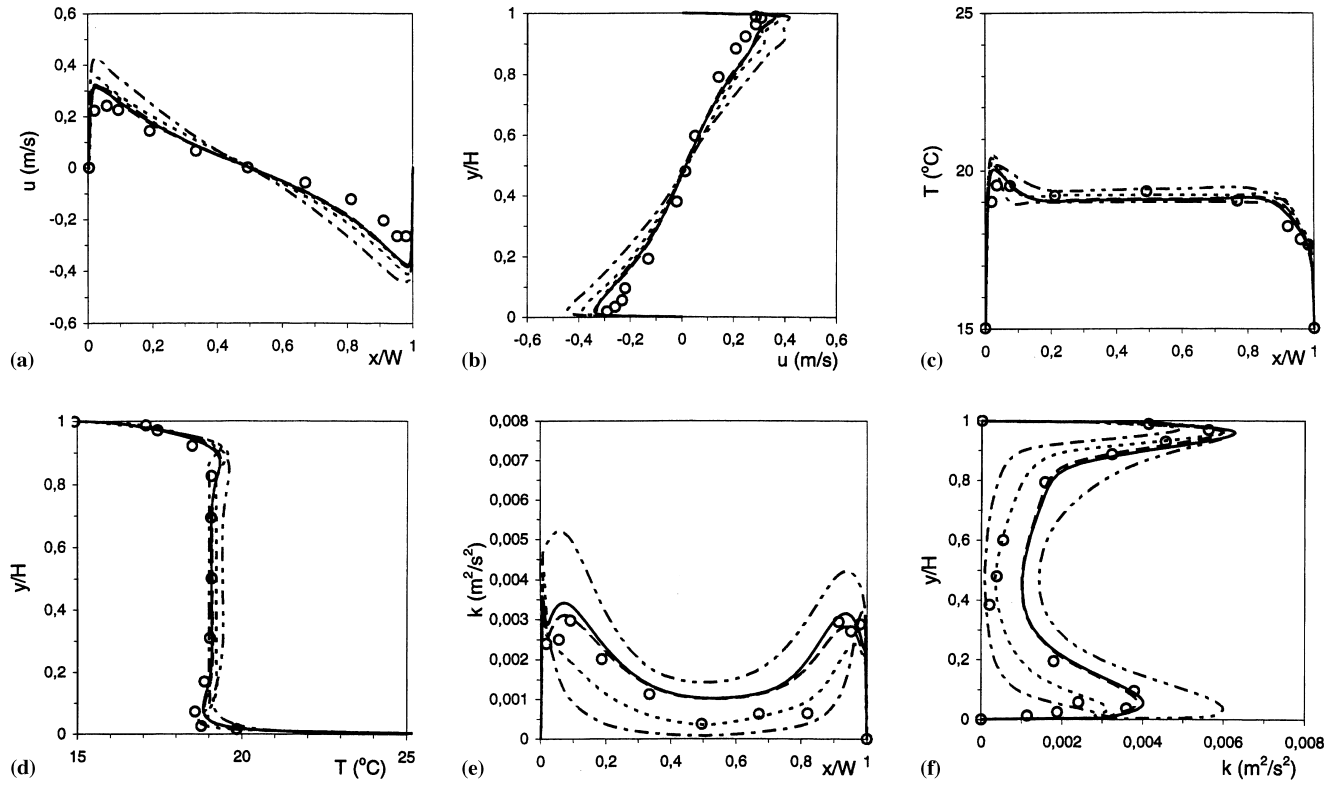

Fig. 7. Comparison of different models for the mixed convection flow in a square cavity. (- · · · -) AKN model, (- · -) LB model, (· · · · · · · · ·) WX model, (– – –) PDH model, (——) PDH + D model, (○) Experiment. (a) Mean velocity at $y = H/2$. (b) Mean velocity at $x = W/2$. (c) Mean temperature at $y = H/2$. (d) Mean temperature at $x = W/2$. (e) Turbulence energy at $y = H/2$. (f) Turbulence energy at $x = W/2$.

5. Conclusions

The performance of LRN k-ω models was investigated for predicting buoyancy affected convection flows in cavities through comparisons with LRN k-ε models and with experimental data. To remove the grid-dependence problem in transition prediction for cavity flows, the simple SGDH model was used in conjunction with a damping function as proposed in this work. Using the present approach in the LRN k-ω model, the rationale for modelling the transition onset in the natural convection boundary layer flow was analyzed.

For the natural convection flow in a tall cavity at a moderate Rayleigh number, $\mathrm{Ra} \approx 5 \times 10^{10}$, all the LRN k-ε and k-ω models considered exhibit strong sensitivity to grid refinement in predicting the transitional boundary layer flow along the vertical wall. Refining grid leads to a delayed transition onset and erroneous results in the predictions. When the grid is refined sufficiently, these models eventually return a laminar solution. None of the models is able to produce a grid-independent solution. It was detected that the grid sensitivity originates from the buoyant source term, G_k, in the k-equation.

Accounting for the buoyant effect on turbulence evolution in the boundary layer, the mechanism for predicting transition onset with the k-ω model was analyzed through some arguments on the net productions per unit dissipation term in the turbulent transport equations by means of a similarity transformation. It was shown that the height of transition onset along a heated vertical wall is inversely proportional to the Rayleigh number. For the cavity flow considered, it was found that transition occurs as the near-wall maximum production of k is brought up to 4–5 times the dissipation.

Using the SGDH model alone, the buoyancy-related term in the k-equation is over-amplified (with negative values) in the neighboring outer region of the boundary layer before transition occurs. Refining grid will reinforce this over-amplification. The buoyant source term plays a significant role as an energy destruction term in the outer region. The near-wall shear production diffuses energy towards the outer region so as to compensate for this destruction. On the other hand, extra shear production is needed to enhance the turbulence in the boundary layer and to trigger transition. If the model over-amplifies (negatively) G_k so that the capability of the shear production cannot become large enough to accommodate the compensation, the turbulence evolution in the boundary layer will not go further, or even the local maximum production may be reduced below a certain level necessary to induce transition. As a result, the transition onset is delayed, or is suppressed at all.

The over-amplification for G_k can be eliminated by using a damping function in the SGDH. When the normalized buoyant production (negative), N_{kb}, in the outer region is reduced so that $|N_{kb}|_{\max}$ is generally smaller than $(N_{ks})_{\max}$ in the boundary layer, the shear production will then possess extra capability to enhance turbulence and lead to a transition onset in the boundary layer as desired. A well-behaved damping function was devised, which is able to appropriately suppress the capacity of G_k for absorbing too much turbulence energy from the boundary layer to the outer region. By means of this approach, the grid-independent solution can be asymptotically achieved. In addition, the use of the damping function enables the rendering of a correct asymptotic behavior for G_k near the vertical walls.

The present method is able to produce reasonable predictions for the cases considered and remove the undesirable grid-dependence problem in transition prediction. For the flow with unstable thermal stratification, it was found that the use of a damping function has insignificant consequence on the prediction as compared with that produced by the same model without employing the damping function. The present approach is expected to be applicable also for other LRN two-equation models, e.g. LRN k-ε models, when they are used to handle similar flow situations.

Appendix A

The damping functions for the LRN turbulence models used in this work are given below.

The Lam–Bremhorst model (LB model)

$$f_\mu = [1 - \exp(-0.0165 R_y)]^2 \left(1 + \frac{20.5}{R_t}\right),$$

$$f_1 = 1 + \left(\frac{0.05}{f_\mu}\right)^3, \quad f_2 = 1 - \exp(-R_t^2).$$

The Abe–Kondoh–Nagano model (AKN model):

$$f_\mu = \left[1 - \exp\left(-\frac{R_\varepsilon}{14}\right)\right]^2 \left\{1 + \frac{5}{R_t^{0.75}} \exp\left[-\left(\frac{R_t}{200}\right)^2\right]\right\},$$

$$f_1 = 1.0,$$

$$f_2 = \left[1 - \exp\left(-\frac{R_\varepsilon}{3.1}\right)\right]^2 \left\{1 - 0.3 \exp\left[-\left(\frac{R_t}{6.5}\right)^2\right]\right\}.$$

The Wilcox model (WX model):

$$f_\mu = \frac{0.025 + R_t/6}{1 + R_t/6}, \quad f_1 = \frac{0.1 + R_t/2.7}{(1 + R_t/2.7)} f_\mu^{-1},$$

$$f_k = \frac{0.278 + (R_t/8)^4}{1 + (R_t/8)^4}.$$

The Peng–Davidson–Holmberg model (PDH model):

$$f_\mu = 0.025 + \left\{1 - \exp\left[-\left(\frac{R_t}{10}\right)^{0.75}\right]\right\} \times \left\{0.975 + \frac{0.001}{R_t} \exp\left[-\left(\frac{R_t}{200}\right)^2\right]\right\},$$

$$f_1 = 1 + 4.3 \exp\left[-\left(\frac{R_t}{1.5}\right)^{0.5}\right],$$

$$f_k = 1 - 0.722 \exp\left[-\left(\frac{R_t}{10}\right)^4\right].$$

In the above damping functions, R_t is the turbulent Reynolds number, $R_t = k^2/(\varepsilon\nu)$ for the k-ε model, and $R_t = k/(\omega\nu)$ for the k-ω model. The quantities R_y and R_ε are defined as: $R_y = k^{1/2} y/\nu$ and $R_\varepsilon = (\nu\varepsilon)^{1/4} y/\nu$, where y is the normal distance to the wall surface.

References

Abe, K., Kondoh, T., Nagano, Y., 1994. A new turbulence model for predicting fluid flow and heat transfer in separating and reattaching flows – I: Flow field calculations. International Journal of Heat and Mass Transfer 37, 139–151.

Bergstrom, D.J., Huang, X., 1997. LES of buoyant cavity flow: Challenge for subgrid scale models. In: K. Hanjalic, T.W.J. Peeters (Eds.), Proceedings of the Second International Symposium on Turbulence, Heat and Mass Transfer, Delft University Press, Delft, pp. 421–430.

Blay, D., Mergui, S., Niculae, C., 1992. Confined turbulent mixed convection in the presence of a horizontal buoyant wall jet. Fundamentals of Mixed Convection, HTD 213, ASME.

Bowles, A., Cheesewright, R., 1989. Direct measurement of the turbulence heat flux in a large rectangular air cavity. Experimental Heat Transfer 2, 59–69.

Cebeci, T., Khattab, A., 1975. Prediction of turbulent-free-convective-heat transfer from a vertical flat plate. ASME Journal of Heat Transfer 469–471.

Cheesewright, R., King, K.J., Ziai, S., 1986. Experimental data for the validation of computer codes for the prediction of two-dimensional buoyant cavity flows. In: J.A.C. Humphrey, C.T. Avedisian, B.W. Le Tourneau, M.M. Chen (Eds.), Significant Questions in Buoyancy Affected Enclosure or Cavity Flows, HTD 60, ASME, pp. 75–81.

Chien, K.Y., 1982. Prediction of channel and boundary layer flows with a low-Reynolds-number turbulence model. AIAA Journal 20, 33–38.

Davidson, L., 1990a. Calculation of the turbulent buoyancy-driven flow in a rectangular cavity using an efficient solver and two different low-Reynolds number k-ε models. Numerical Heat Transfer 18, 129–147.

Davidson, L., 1990b. Second-order corrections of the k-ε model to account for non-isotropic effects due to buoyancy. International Journal of Heat and Mass Transfer 33, 2599–2608.

Davidson, L., Farhanieh, B., 1992. CALC-BFC: A finite-volume code employing collocated variable arrangement and Cartesian velocity components for computation of fluid flow and heat transfer in complex three-dimensional geometries. Report 92/4, Department of Thermo and Fluid Dynamics, Chalmers University of Technology, Gothenburg, Sweden.

Davidson, L., 1992. Computation of natural-convection flow in a square cavity. In: R.A.W.M. Henkes, C.J. Hoogendoorn (Eds.), Turbulent Natural Convection in Enclosures, Proc. Eurotherm Seminar vol. 22, Delft, The Netherlands, pp. 43–53.

Giel, P.W., Schmidt, F.W. 1986. An experimental study of high Rayleigh number natural convection in an enclosure. In: C.L. Tien, V.P. Carey, J.K. Ferrell (Eds.), Heat Transfer, vol. 4, pp. 1459–1464.

Hanjalic, K., Vasic, S., 1993. Computation of turbulent natural convection in rectangular enclosures with an algebraic flux model. International Journal of Heat and Mass Transfer 36, 3603–3624.

Heindel, T.J., Ramadhyani, S., Incropera, F.P., 1994. Assessment of turbulence models for natural convection in an enclosure. Numerical Heat Transfer 26 (Part B), 147–172.

Henkes, R.A.W.M., 1990. Natural-convection boundary layers. Ph.D. thesis, Delft University, The Netherlands.

Henkes, R.A.W.M., van Der Vlugt, F.F., Hoogendoorn, C.J., 1991. Natural-convection flow in a square cavity calculated with low-Reynolds-number turbulence models. International Journal of Heat and Mass Transfer 34, 377–388.

Henkes, R.A.W.M., Hoogendoorn, C.J., 1995. Comparison exercise for computations of turbulent natural convection in enclosures. Numerical Heat Transfer 28 (Part B), 59–78.

Henkes, R.A.W.M., Le Quéré, P., 1996. Three-dimensional transition of natural-convection flows. Journal of Fluid Mechanics 319, 281–303.

Ince, N.Z., Launder, B.E., 1989. On the computation of buoyancy-driven turbulent flows in rectangular enclosures. International Journal of Heat and Fluid Flow 10, 110–117.

Incropera, F.P., DeWitt, D.P., 1990. Fundamentals of Heat and Mass Transfer. Wiley, New York.

Lam, C.K.G., Bremhorst, K., 1981. A modified form of the k-ε model for predicting wall turbulence. ASME Journal of Fluid Engineering 103, 456–460.

Le Quéré, P., 1992. An improved Chebyshev collocation algorithm for direct simulation of 2D turbulent convection in differentially heated cavities. In: Proceedings of the International Conference on Spectral Higher Order Methods, Montpellier, France.

Markatos, N.C., Malin, M.R., Cox, G., 1982. Mathematic modelling of buoyancy-induced smoke flow in enclosures. International Journal of Heat and Mass Transfer 25, 63–75.

Markatos, N.C., Pericleous, K.A., 1984. Laminar and turbulent natural convection in an enclosed cavity. International Journal of Heat and Mass Transfer 27, 755–772.

Murakami, S., Kato, S., Chikamoto, T., Laurence, D., Blay, D., 1996. New low-Reynolds-number k-ε model including damping effect due to buoyancy in a stratified flow field. International Journal of Heat and Mass Transfer 39, 3483–3496.

Paolucci, S., Chenoweth, D.R., 1989. Transition to chaos in a differentially heated vertical cavity. Journal of Fluid Mechanics 201, 379–410.

Peng, S.-H., Davidson, L., Holmberg, S., 1997. A modified low-Reynolds-number k-ω model for recirculating flows. ASME Journal of Fluid Engineering 119, 867–875.

Peng, S.-H., 1998. Modelling of turbulent flow and heat transfer for building ventilation. Ph.D. thesis, Chalmers University of Technology, Gothenburg, Sweden.

Rodi, W., 1984. Turbulence Models and Their Application in Hydraulics – A State of the Art Review. University of Karlsruhe, Germany.

Savill, A.M., 1996. One-point closures applied to transition. In: M. Hallbäck, D.S. Henningson, A.V. Johansson, P.H. Alfredsson (Eds.), ERCOFTAC Series II: Turbulence and Transition Modelling, Kluwer Academic Publishers, Dordrecht, pp. 233–268.

So, R.M.C., Sommer, T.P., 1994. A near-wall eddy conductivity model for fluids with different Prandtl numbers. ASME Journal of Fluid Engineering 116, 844–854.

To, W.M., Humphrey, J.A.C., 1986. Numerical simulation of buoyant, turbulent flow – I. Free convection along a heated vertical flat plate. International Journal of Heat and Mass Transfer 29, 573–592.

van Leer, B., 1974. Towards the ultimate conservative difference scheme: Monotonicity and conservation combined in a second-order scheme. Journal of Computational Physics 14, 361–370.

White, F.M., 1974. Viscous Fluid Flow. McGraw-Hill, New York.

Wilcox, D.C., 1994. Simulation of transition with a two-equation turbulence model. AIAA Journal 32, 247–254.